Evidence of midgap-state-mediated transport in 45° symmetric [001] tilt YBa$_2$Cu$_3$O$_{7-x}$ bicrystal grain-boundary junctions

G. Testa, E. Sarnelli, A. Monaco, and E. Esposito

Istituto di Cibernetica "E. Caianiello" del CNR, Via Campi Flegrei 34, I-80078 Pozzuoli (Naples), Italy

M. Ejrnaes

INFN-Napoli, Via Cintia, I-80126 Naples, Italy

D.-J. Kang

*Nanoscience Centre, IRC in Nanotechnology, University of Cambridge, Cambridge CB3 0FF, United Kingdom
and Sungkyunkwan Advanced Institute of Nanotechnology and Department of Physics, Sungkyunkwan University, Suwon 440-746 Korea*

S. H. Mennema, E. J. Tarte, and M. G. Blamire

Department of Materials Science, University of Cambridge, Pembroke Street, Cambridge, CB2 3QZ United Kingdom

We have investigated the effect of midgap bound states on the Josephson properties of symmetric 45° [001] tilt bicrystal grain-boundary junctions (GBJ's) characterized by different junction widths. GBJ's, 1 μm wide, show a monotonic temperature dependence of the Josephson current with a slight upwards curvature, the result of the competition between midgap states and the opposite-sign continuous current. In some junctions, an increasing contribution of the midgap-state-mediated current is observed at low temperatures, leading to an anomalous nonmonotonic temperature dependence of the critical current. This behavior is more evident for junctions smaller than 500 nm, where, in some cases, a 0- to π-junction transition is clearly observed. Experimental results agree qualitatively with theoretical models taking into account midgap states in strongly nonuniform barrier interfaces.

I. INTRODUCTION

One of the most interesting debates in condensed matter physics is the discussion about the symmetry of the superconducting wave function in high-critical-temperature (HTS) cuprates.[1–4] In recent years, a number of experiments have given clear evidence of an unconventional d-wave order parameter symmetry, characterized by a strongly anisotropic order parameter with nodes along the (110) directions in k space and a sign change (corresponding to a π-phase shift of the superconducting wave function) between orthogonal k_x and k_y directions. The most interesting results have been obtained by phase-sensitive tests,[5–8] mainly based on superconducting loops containing one or more junctions, capable of distinguishing between d-wave and asymmetric s-wave symmetries.

Another powerful phase-sensitive test is based on the property of d-wave superconductors to form superconducting bound surface states at the Fermi energy, the so-called midgap states (MGS's).[9,10] Such MGS's, completely absent in conventional s-wave superconductors, are generated by the combined effect of Andreev reflections[11] and the directional sign change associated with the d-wave order parameter symmetry. MGS's have been observed experimentally as a zero-bias conductance peak (ZBCP) in superconducting/insulating/normal-metal (SIN) and superconducting/insulating/superconducting (SIS) junctions and in the impurity induced zero-energy density of states by scanning tunneling microscopy measurements.[12–16] One of the most striking consequences of MGS's is the prediction of an

anomalous temperature dependence of the Josephson current $I_C(T)$,[17–20] strongly dependent on the barrier transparency and on the misorientation angles α_i ($i=1,2$) between the crystallographic axes of the two electrodes and the direction normal to the interface (Fig. 1). In particular, a transition from a 0 to π junction with decreasing temperature has been theoretically predicted in 45° symmetric [001] tilt grain-boundary junctions (GBJ's).[17–20]

Experimentally, the observation of such a 0-π transition is made very difficult by the large faceting typical of HTS GBJ's and, more generally, by the complex structure of the barrier interface, characterized by many high transmissivity channels.[21–23]

The first experimental evidence of a nonmonotonic temperature dependence was achieved by current-phase relation measurements in submicron 45° [001] tilt symmetric bicrystal GBJ's.[24] However, that experiment did not reveil a π-phase shift of the ground state but instead a transition
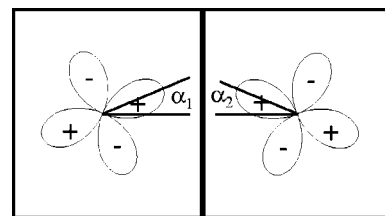

FIG. 1. Schematic geometry of the grain-boundary interface. α_1 and α_2 are the angles between the normal to the interface and the crystallographic axes on the left and right sides, respectively.

from a 0 state to a double-degenerate ground state, characterized by two minima of the free energy at $\varphi = \pm\varphi_0$, with $0 < \varphi_0 < \pi$.

Very recently, the 0-π junction crossover with temperature has been finally observed by using a double phase-sensitive test.[25] Transport measurements of a dc superconducting quantum interference device (SQUID) with two submicron 45° symmetric GBJ's showed both an anomalous nonmonotonic temperature dependence of the Josephson current and a half-flux quantum shift in the magnetic flux modulation of the SQUID critical current.

In this paper, we are going to investigate the influence of the junction width on the temperature dependence of the Josephson current in symmetric 45° [001] tilt bicrystal GBJ's. The different $I_C(T)$ behaviors observed will be compared with the theoretical model described in Ref. 17 by also including the influence of strongly non uniform barrier interfaces.

II. THEORETICAL DESCRIPTION

Defining θ as the angle between the quasiparticle trajectory and the normal to the grain boundary interface, the order parameter sensed by a quasiparticle incident on the barrier is $\Delta_i(\theta) = \Delta(0)\cos[2(\theta - \alpha_i)]$. In 45° symmetric junctions, MGS's exist in both electrodes only if quasiparticles probe different signs of the order parameter before and after the reflection—i.e., only within limited intervals of the angle θ, $\theta/8 < |\theta| < 3\theta/8$. For other angles, the behavior is similar to that of *s*-wave superconductors. Because of the coupling between the two electrodes, MGS energies are split and shifted according to the junction phase difference φ and the barrier transparency D, where $0 < D < 1$.[17] In 45° GBJ's, the lower MGS energy level is characterized by a shift of π in the ground state. As a consequence, the contribution of MGS's, $I_{MGS}(\varphi)$, to the total Josephson current $I_T(\varphi)$ is opposite to the continuous state current $I_{CONT}(\varphi)$, whose equilibrium phase difference is $\varphi = 0$ as in conventional *s*-wave supercon-

ductors. This effect is more evident at very low temperatures when mainly the lower-energy level is populated. It is worth noting that $I_{MGS}(\varphi)$ is proportional to the square root of the barrier transparency, $\sqrt{D}$, as in any resonant coupling phenomena,[26] while $I_{CONT}(\varphi)$ is proportional to D. Therefore, the contribution of MGS's strongly depends on the barrier transparency.

Formally, the Josephson current of high-critical-temperature grain-boundary junctions has often been described in the literature by using the well-known Sigrist-Rice formula[27,28] $J_C = A \cos 2\alpha_1 \cos 2\alpha_2$, successfully applied in a number of experiments testing the order parameter symmetry. Tsuei and co-workers were able, by using this formula, to design superconducting loops with an odd number of π junctions, characterized by a π-phase shift in the electronic ground state.[6,7] The Sigrist-Rice formula, including not only the in-plane angles α_1 and α_2 but also the 45° out-of-plane rotation of one of the two electrodes, was also successfully used to describe the dependence of the Josephson current on the interface orientation in [100] tilt biepitaxial grain-boundary junctions.[29] However, this formula does not take into account the presence of MGS's and describes the Josephson current only for quasiparticle trajectories approximately perpendicular to the barrier. In order to include both the intrinsic phase of the pair potential and the formation of localized states at the interface, a tunneling cone has to be considered, whose amplitude is dependent on the barrier transparency.[17,18]

In this paper, we will follow the theoretical approach described in Ref. 17. Assuming a rectangular barrier with thickness d_i and height U_0, Tanaka and Kashiwaya derived the following $I(\varphi)$ dependence (TK equation):

$$R_n I(\varphi) = \frac{\pi R_n^* K_B T}{e} \left\{ \sum_n \int_{-\pi/2}^{\pi/2} F(\theta, i\omega_n, \varphi) \sin(\varphi)\sigma_n \cos(\theta)d\theta \right\},$$
(1)

where

$$F(\theta, i\omega_n, \varphi) = \frac{\eta_{L+}\eta_{R+}|(1-\sigma_n)\Gamma_1(\theta, i\omega_n)\Gamma_2(\theta, i\omega_n) + \sigma_n|\Gamma_3(\theta, i\omega_n, \varphi)|^2|}{|(1-\sigma_n)\Gamma_1(\theta, i\omega_n)\Gamma_2(\theta, i\omega_n) + \sigma_n\Gamma_3(\theta, i\omega_n, \varphi)\Gamma_4(\theta, i\omega_n, \varphi)|^2},$$

$$\Gamma_1(\theta, i\omega_n) = 1 + \eta_{L+}\eta_{L-}, \quad \Gamma_2(\theta, i\omega_n) = 1 + \eta_{R+}\eta_{R-},$$

$$\Gamma_3(\theta, i\omega_n, \varphi) = 1 + \eta_{L-}\eta_{R-}\exp(-i\varphi),$$

$$\Gamma_4(\theta, i\omega_n, \varphi) = 1 + \eta_{L+}\eta_{R+}\exp(i\varphi),$$

$$\eta_{L(R)\pm} = \frac{\Delta_{L(R)}(\Theta_\pm)}{\omega_n + \Omega_{n,L(R)\pm}}, \quad \Omega_{n,L(R)\pm} = \text{sgn}(\omega_n)\sqrt{\Delta_{L(R)}^2(\Theta_\pm) + \omega_n^2},$$

$$2D = 1/R_n^* = \int_{-\pi/2}^{\pi/2} \sigma_n \cos(\theta)d\theta,$$

$$\sigma_n = \frac{4Z_\theta^2}{(1-Z_\theta^2)^2 \sinh^2(\lambda d_i) + 4Z_\theta^2 \cosh^2(\lambda d_i)},$$

$$\lambda = \lambda_0 \sqrt{1 - \kappa^2 \cos^2(\theta)}, \quad Z_\theta = \frac{\kappa \cos(\theta)}{\sqrt{1 - \kappa^2 \cos^2(\theta)}},$$
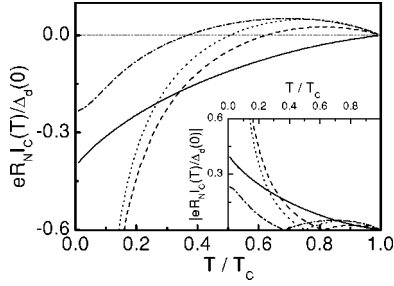
FIG. 2. Theoretical $I_C(T)$ dependence for 45° symmetric [001] tilt GBJ's with different barrier transparencies: solid line ($\kappa=0.5$, $\lambda_0 d_i=0$, $D=1/2R_n^*=1$), dashed line ($\kappa=0.5$, $\lambda_0 d_i=3$, $D=10^{-2}$), dotted line ($\kappa=0.5$, $\lambda_0 d_i=5$, $D=2.8\times10^{-4}$), and dash-dotted line ($\kappa=0.5$, $\lambda_0 d_i=5$, $\gamma=0.1\Delta(0)$, $D=2.8\times10^{-4}$). The inset shows the absolute value of the critical current, as it would be extracted by direct transport measurements.

$$\omega_n = 2\pi k_B T(n+1/2) + \text{sgn}(\omega_n)\gamma.$$

In these equations, σ_n represents the tunneling conductance for injected quasiparticles in the normal state, $\Delta_{L(R)}$ the absolute value of the pair potential in the left (right) electrode, and γ the lifetime broadening of quasiparticles due to surface roughness. The two parameters affecting the barrier transparency D are $\kappa=K_F/\lambda_0$ and $\lambda_0 d_i$, where K_F is the Fermi momentum and $\lambda_0=\sqrt{(2mU_0/\hbar^2)}$, with U_0 the Hartree potential at the interface. Equation (1) gives the current-phase relation as a function of the temperature for a fixed misorientation angle. As reported in Ref. 17, $I(\varphi)$ can be decomposed as $I(\varphi)=\Sigma_n[I_n\sin(n\varphi)+J_n\cos(n\varphi)]$, where $J_n=0$ if time-reversal symmetry is not broken. The harmonic components with $n>1$ are calculated in Eq. (1) as the contributions of the nth-reflection processes of quasiparticles. By maximizing $I(\varphi)$ for different temperatures, it is then possible to obtain the theoretical temperature dependence of the critical current $I_C(T)$ for different GBJ configurations.

Figure 2 shows the $I_C(T)$ dependence predicted for 45° symmetric [001] tilt GBJ's characterized by the same $\kappa=0.5$ and different $\lambda_0 d_i$ values, corresponding to different barrier transparencies D. The solid line shows the behavior expected for a high-transparency junction ($\kappa=0.5$, $\lambda_0 d_i=0$, $D=1/2R_n^*=1$); in this case, the midgap-state-mediated current is already dominant at a temperature close to the critical one and the total Josephson current is negative in the whole temperature range. The absolute value $|I_C(T)|$ is monotonic with a slight upwards curvature (inset of Fig. 2). The dashed line refers to the case $\kappa=0.5$, $\lambda_0 d_i=3$, $D=10^{-2}$ and the dotted line to $\kappa=0.5$, $\lambda_0 d_i=5$, $D=2.8\times10^{-4}$. In these two junction configurations the barrier transparency is much smaller and the MGS-mediated current dominates only at lower temperatures. A crossover from a positive to a negative current, corresponding to a "0"-"π" transition, is then expected at a transition temperature T^*. Of course, the $|I_C(T)|$ value, as would be extracted by direct transport measurements, is clearly nonmonotonic. Finally, the dash-dotted line shows the theoretical behavior for $\kappa=0.5$, $\lambda_0 d_i=5$, $D=2.8\times10^{-4}$ when a quasiparticle lifetime broadening $\gamma=0.1\Delta(0)$ is included as well. The resulting effect is a saturation of the critical current
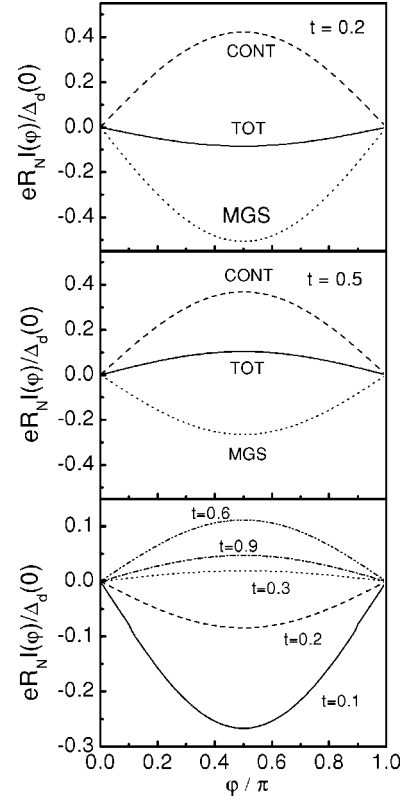

FIG. 3. Current-phase relations for the configuration [$\kappa=0.5$, $\lambda_0 d_i=5$, $D=1/2R_n^*=2.8\times10^{-4}$, $\gamma=0.1\Delta(0)$] at two different normalized temperatures $t=T/T_C=0.2$ (a) and 0.5 (b), respectively. Dashed lines show $R_n I_{CONT}(\varphi)$, dotted lines $R_n I_{MGS}(\varphi)$, and solid lines $R_n I_T(\varphi)$. (c) Current-phase relation of $R_n I_T(\varphi)$ for several normalized temperatures $t=0.1, 0.2, 0.3, 0.6, 0.9$.

at low temperatures, corresponding to a smaller weight of the MGS-mediated current, and a shift of the crossover temperature towards lower T.

In Figs. 3(a) and 3(b) we show, for the latter configuration, the different contributions to the total Josephson current $R_n I_T(\varphi)$ (solid line) at two normalized temperatures $t=T/T_C=0.2$ and 0.5, respectively. Dashed lines represent the continuous contribution $R_n I_{CONT}(\varphi)$ and dotted lines the opposite-sign MGS-mediated current $R_n I_{MGS}(\varphi)$ (the procedure used to calculate $R_n I_{CONT}(\varphi)$ and $R_n I_{MGS}(\varphi)$ is reported in Ref. 17). Figure 3(c) shows the current-phase relation of $R_n I_T(\varphi)$ for several temperatures, from $t=0.1$ to $t=0.9$. A transition from a $\sin(\varphi)$ to a $\sin(\varphi+\pi)$ dependence, with a π-phase shift, is clearly observed at a crossover temperature $T^*\approx0.3T_C$.

It is worth noting that the same T^* can be obtained with different combinations of κ and $\lambda_0 d_i$, corresponding to different values of the barrier transparency D, as observed in Fig. 4 for three values of γ: $\gamma=0$, $0.1\Delta(0)$, and $0.2\Delta(0)$. The different symbols relate to different κ values: squares, $\kappa=0.2$; circles, $\kappa=0.4$, triangles, $\kappa=0.6$; and rhombs, $\kappa=0.8$.

III. EXPERIMENTAL PROCEDURES

A. Sample fabrication

All the measurements that will be discussed in the present paper relate to submicron, symmetric 45° [001] tilt bicrystal
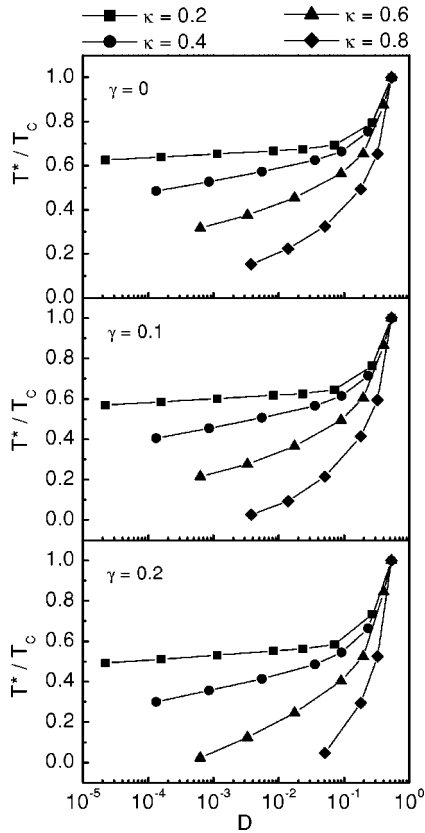
FIG. 4. Dependence of T^* on the barrier transparency D for three γ values $\gamma=0$, $0.1\Delta(0)$, $0.2\Delta(0)$. Squares relate to $\kappa=0.2$, circles to $\kappa=0.4$, triangles to $\kappa=0.6$, and rhombs to $\kappa=0.8$.

grain-boundary junctions. Their fabrication has been widely described elsewhere,[30] so only an outline of the procedure is reported here.

The samples were fabricated on symmetric 45° [001] tilt SrTiO$_3$ bicrystal substrates. YBa$_2$Cu$_3$O$_{7-x}$ films, 120–140 nm thick, were first deposited by laser ablation. An amorphous SrTiO$_3$ layer was then laser ablated over the bicrystal line, in order to passivate the junction and protect the YBa$_2$Cu$_3$O$_{7-x}$ surface from gallium contamination during the focused ion beam (FIB) process. Finally, a thin gold layer was deposited by magnetron sputtering to cover the sample with a conductive layer for the FIB process and to prevent the degradation of the YBa$_2$Cu$_3$O$_{7-x}$ surface in the contact area during photolithographic processes.

The device pattern was achieved by standard photolithography and a water-cooled argon ion milling etch. To reduce junction widths, YBa$_2$Cu$_3$O$_{7-x}$ was removed from the junction area by a FIB microscope with a Ga source. Contact areas were finally obtained by depositing additional 50 nm of gold by magnetron sputtering. Following this procedure, we have fabricated several GBJ's and SQUID's with widths in the range 0.3–1 μm. Figure 5 shows the FIB picture of a 350-nm-wide grain-boundary junction, just after the focused ion beam etch (the dashed line indicates the bicrystal line, not visible under the FIB).

B. Experimental technique

All the experiments have been made, with very-low-noise electronics, in a helium cryostat shielded by 1-mm-thick alu-
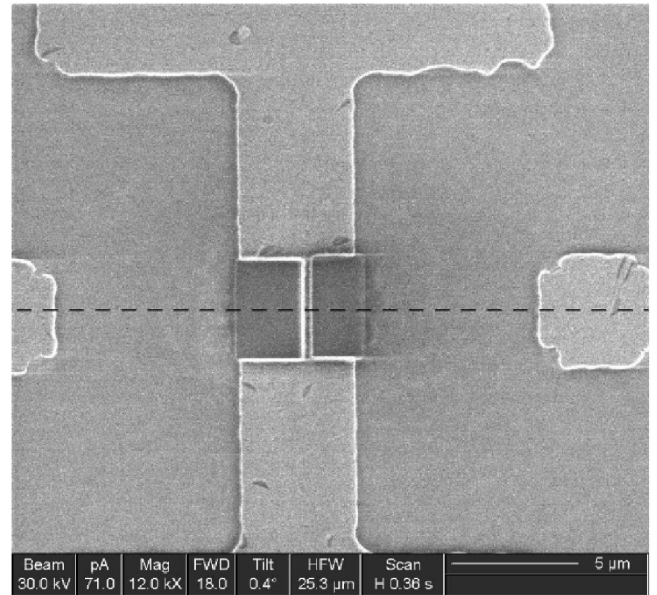

FIG. 5. FIB picture of a 350-nm-wide GBJ (the dashed line indicates the bicrystal line, not visible by FIB).

minum and three mu-metal shields with a residual field lower than 1 mG. Current-voltage (I-V) characteristics have been measured as a function of the temperature, from 300 mK to T_C by using two different vacuum probes: the first, with a heating element, capable of stabilizing the temperature in the range from 300 mK to 4.2 K; the second, also equipped with a heating element, working in the range from 4.2 K to T_C and covered by two additional shields, made of cryoperm and superconducting lead, respectively. Samples have also been measured without any heaters, in helium vapors, by carefully controlling their distance from the helium bath, in order to rule out any possible noises or flux trappings arising from the coupling between heater and signal wires.

IV. EXPERIMENTAL RESULTS AND DISCUSSION

In this section we analyze the experimental results obtained from submicron GBJ's fabricated with different widths. At $T=4.2$ K, all the junctions show critical current densities J_C of the order of $3-5\times10^3$ A/cm^2 and I_CR_n products, with R_n the asymptotic normal resistance, in the range 300–500 μV. The estimated Josephson penetration length[30] is of the order of 20 μm, much larger than all of the junction widths. Figure 6 shows the I-V characteristic of a typical submicron GBJ at $T=4.2$ K. It is characterized by a resistively-shunted-junction- (RSJ-like) behavior[31] with a small hysteresis, mainly due to the capacitance of the SrTiO$_3$ substrate. In the inset, the magnetic field dependence of the Josephson current, characterized by a Fraunhofer-like modulation pattern, is also reported.

Figure 7 shows the normalized temperature dependence of the Josephson current for a 920-nm-wide GBJ. $I_C(T)$ is monotonic, with a slight upwards curvature, and tends to a saturation at low temperature (down to 300 mK). The junction normal resistance is constant in the whole temperature
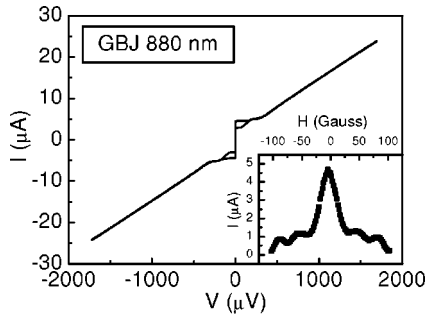
FIG. 6. *I-V* characteristics of a 880-nm-wide junction at $T = 4.2$ K. The inset shows the magnetic field dependence of the Josephson current for the same GBJ.

FIG. 8. Temperature dependence of the Josephson current for a 880-nm-wide GBJ (squares). The solid line is only a guide to the eye. The inset shows the low-temperature region (0.3–4.2 K) in detail.

range. This behavior is typical for most of the measured junctions with widths of the order of 1 μm. Similar results were also reported for $YBa_2Cu_3O_{7-x}$ ramp-edge junctions with electrodes relatively rotated by 45° and characterized by different *a-b* plane orientations.[32]

Experimental data can be well accounted for by Eq. (1), taking also into account a finite quasiparticle lifetime. The solid line corresponds to the theoretical curve obtained with the following parameters: $\Delta(0)=0.018$ eV, $\kappa=0.175$, $\lambda_0 d_i = 0.25$, and $\gamma=0.1\Delta(0)$. For comparison, the curve obtained with the same parameters but $\gamma=0$ (perfect interface) is also shown (dashed line). In the latter case, the theoretical upwards curvature is much larger, indicating that the effect of MGS's at low temperatures would be strongly enhanced by reducing the surface roughness. It is worth noting that the comparison with the TK equation has only a qualitative meaning because of the presence of too many free parameters $[\kappa, \lambda_0 d_i, \Delta(0), \gamma]$. Moreover, simulations do not take into account the presence of faceting at the grain boundary interface and the inhomogeneity of the barrier interface, which strongly suppress the effect of MGS's.

The experimental monotonic temperature dependence implies that $T^*/T_C=1$. As shown in Fig. 4, a barrier transparency D of about 0.5 represents a threshold between monotonic and nonmonotonic behaviors, independently of κ, $\lambda_0 d_i$, and γ. We can therefore estimate that D is larger than 0.5 in
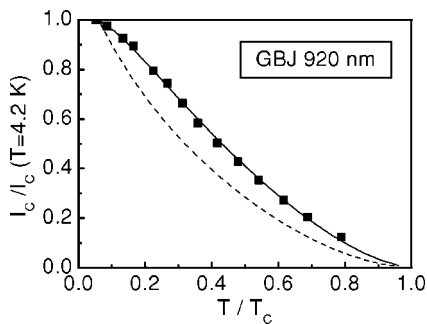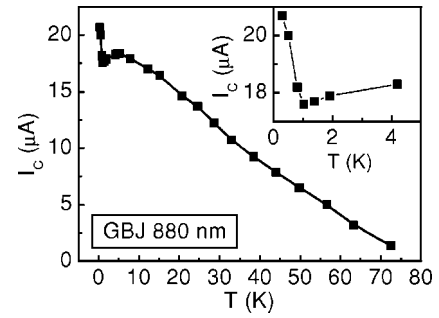

FIG. 7. Normalized temperature dependence of the Josephson current for the 920-nm-wide GBJ (squares). The theoretical curves have been obtained by using the TK formula with $\gamma=0.1\Delta(0)$ (solid line) and $\gamma=0$ (dashed line); in both cases, $\Delta(0)=0.018$ eV, $\kappa=0.175$, $\lambda_0 d_i=0.25$.

this case. This value is much larger than the average barrier transparency D_{ave}, about $1-2\times10^{-3}$, estimated by the normal resistance value $\rho_{ab}l/R_nA$,[33] where ρ_{ab} (resistivity in the *a-b* plane) is assumed to be 10^{-4} Ω cm and l, the mean free path, equal to 10 nm. As already pointed out in Ref. 16, the difference between the two transparency estimates can be explained considering the nonuniform barrier interface, typical of HTS grain-boundary junctions. Indeed, while the D value obtained by MGS measurements is mainly influenced by the high-transparency regions, D_{ave}, which is calculated from the measured normal resistance, is averaged over the whole junction interface.

In some GBJ's, in spite of the very similar junction width, we have observed a completely different temperature dependence of the Josephson current. Figure 8 shows, for example, the $I_C(T)$ dependence for a 880-nm-wide junction. By decreasing the temperature, from T_C to 300 mK, $I_C(T)$ first increases, then slightly decreases at about 4.5 K, and finally increases again at very low T ($T<4.2$ K). The total behavior is clearly nonmonotonic, recalling, in some ways, that observed by inductive measurements on submicron bicrystal junctions.[24] In that case, it was explained as the result of a large second-harmonic component (SHC) which prevented observing a π-phase shift in the junction ground state. In order to justify a so-large SHC, the authors introduced the presence of phase fluctuations of the superconducting order parameter.[34]

In comparison with the results reported in Ref. 24, our experimental data show a nonmonotonic behavior appearing at much smaller temperatures ($T^*/T_C\approx0.014$), a critical current value at T^*, $I_C(T^*)$, much larger than 0 (between 0.6 and 0.85 in our junctions), and a very large I_{C2}/I_C ($T=0.05T_C$) ratio, where I_{C2} is the relative maximum of the critical current for $T>T^*$. Such features cannot be explained by assuming a uniform grain boundary, for any choices of the parameters κ and $\lambda_0 d_i$ and therefore for any transparencies D; additional harmonic components alone are thus not able to explain this anomalous $I_C(T)$ behavior. Here, we want to show that such a temperature dependence may be accounted for by Eq. (1) considering a strongly nonuniform barrier interface.

In Fig. 9 we report, as an example, the normalized $I_C(T)$ prediction (solid line) for an inhomogeneous 45° grain-
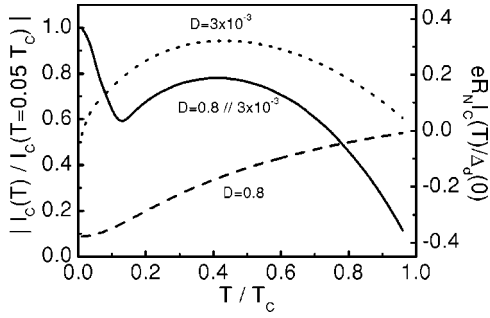
FIG. 9. Left *y* axis: normalized $|I_C(T)/I_C(t=0.05\,T_C)|$ dependence (solid line) for an inhomogeneous 45° grain-boundary junction characterized by a low-transparency barrier, of the order of $D=3 \times 10^{-3}$, with high-transmissivity channels ($D=0.8$); in the calculations, we have assumed that the sum of all the channel widths is about 1/250th of the total GBJ width. Right *y* axis: Theoretical behaviors related to homogeneous GBJ's with $\kappa=0.8$, $\lambda_0 d_i=0.5$, $\gamma=0.1\Delta(0)$, $D=0.8$ (dashed line) and $\kappa=0.8$, $\lambda_0 d_i=5$, $\gamma=0.1\Delta(0)$, $D=3 \times 10^{-3}$ (dotted line), respectively.

boundary junction characterized by a low-transparency barrier *D*, of the order of 3×10^{-3}, with some high-transmissivity point contacts ($D=0.8$). In order to weight properly the two contributions from low- and high-transparency regions, we have taken into account the two different conductance values. Moreover, we have assumed that the sum of all of the high-transparency channel widths is about 1/250th of the total GBJ width. Simulations have been performed with $\kappa=0.8$ to account for the large experimental I_{C2}/I_C ($T=0.05\,T_C$) ratio. The dependence obtained by Eq. (1) for the total GBJ, reported in the figure together with the two separate $I_C(T)R_n$ contributions related to both low- (dashed line) and high- (dotted line) transparency regions, shows a behavior similar to the experimental one.

By further reducing the junction width, we could expect more uniform barrier interfaces with a reduction of the high-transmissivity channels. Figure 10 shows the temperature dependence $I_C(T)$ for a 480-nm-wide junction; it is characterized by a clear nonmonotonic behavior, with a large MGS contribution at low *T* and a crossover temperature at about 0.39 T_C. $I_C(300\text{ mK})$ and T_C are 1.3 μA and 76.2 K, respec-
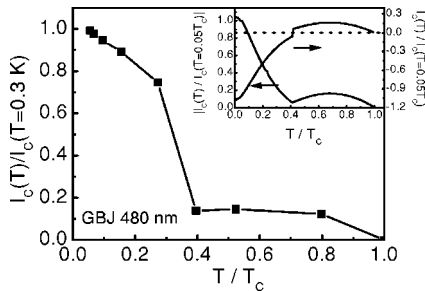

FIG. 10. Temperature dependence of the Josephson current for a 480-nm-wide GBJ (squares). $I_C(300\text{ mK})$ and T_C are 1.3 μA and 76.2 K, respectively. The solid line is only a guide to the eye. The inset shows the theoretical prediction calculated with $\Delta(0)=0.018$ eV, $\kappa=0.8$, $\lambda_0 d_i=2$, and $\gamma=0.1\Delta(0)$ (right *y* axis), together with its absolute value (left *y* axis).
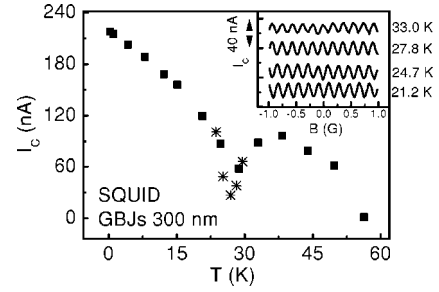

FIG. 11. Temperature dependence of the Josephson current for a dc SQUID with two 300-nm-wide junctions (squares and stars refer to two different sets of measurements). In the inset, the magnetic field dependence of the Josephson current shows a clear 0-π junction transition across T^*.

tively. Such an anomalous $I_C(T)$ dependence is very similar to that recently observed in a dc SQUID with two 300-nm-wide GBJ's.[25] There, $I_C(T)$ became almost zero at $T^* \approx 0.45\,T_C$, increasing for both higher and lower temperatures (Fig. 11). In the inset of Fig. 10, we show the theoretical $I_C(T)$ dependence calculated for $\Delta(0)=0.018$ eV, $\kappa=0.8$, $\lambda_0 d_i=2$, and $\gamma=0.1\Delta(0)$ (right *y* axis), together with its absolute value (left *y* axis). Although there are several differences with the experimental curve, the theoretical curve can approximately account for the experimental behavior in terms of both the value of the crossover temperature T^* and the ratio $I_{C2}/I_C(300\text{ mK})$ (for this GBJ, $T^* \approx 30$ K). At $T=T^*$ the theoretical critical current is not exactly zero and a clear discontinuity appears in the $I_C(T)$ dependence. Such a discontinuity is related to a jump of the phase φ_M, defined as the junction-phase difference giving the maximum value of the current-phase relation $I(\varphi)$.[18,20] It is worth noting that our experimental $I_C(T)$ behavior can also be qualitatively accounted for by different choices of the parameters κ, $\lambda_0 d_i$, and γ. A very important point is, however, that, independently of the true value of such parameters, the transition from a monotonic to a nonmonotonic behavior is due to a decrease of the barrier transparency *D*. Indeed, as shown in Fig. 4, T^* is a decreasing function of *D*, its change depending on the value of the parameter κ. Experimental results are then consistent with the assumption that a reduction of the junction width leads to more uniform grain-boundary interfaces, with smaller local changes; low-transparency barriers may then be achieved more easily, allowing the observation of 0-π junction crossovers with temperature. Recently, this transition has also been confirmed by measurements of the magnetic field dependence of the critical current in a submicron dc SQUID.[25] A half-flux quantum shift in the maximum critical current has been clearly observed, indicating the transition from a 0 loop to a frustrated π loop by decreasing the temperature (inset of Fig. 11).

V. CONCLUSIONS

We have investigated the effect of midgap states on the Josephson current of submicron 45° symmetric [001] tilt bicrystal GBJ's characterized by different widths. For widths

below 1 μm, a nonmonotonic temperature dependence of the critical current sometimes appears. However, a clear transition from positive to negative critical currents is only observed in junctions smaller than 500 nm. This result can be accounted for by considering a nonuniform barrier interface, characterized by regions with different barrier transparencies. By reducing the junction width, more homogeneous interfaces are then expected and low-transparency barriers, leading to 0-π transitions, can be more easily achieved.[24,25,35] It is worth noting that any quantitative fits are made very difficult by additional spurious effects, like faceting or defects at the interface. Additional information on the barrier transparency may be obtained by alternative measurements such as, for instance, quasiparticle conductance spectroscopy.

[1] R. Dagotto, Rev. Mod. Phys. **66**, 763 (1994).

[2] D. J. Scalapino, Phys. Rep. **250**, 330 (1995).

[3] J. Annett, N. Goldenfeld, and A. J. Leggett, in *Physical Properties of High Temperature Superconductors*, edited by D. M. Ginsberg (World Scientific, Singapore, 1996).

[4] V. B. Geshkenbein, A. I. Larkin, and A. Barone, Phys. Rev. B **36**, 235 (1987).

[5] D. J. Van Harlingen, Rev. Mod. Phys. **67**, 515 (1995).

[6] C. C. Tsuei and J. R. Kirtley, Rev. Mod. Phys. **72**, 969 (2000).

[7] J. R. Kirtley, C. C. Tsuei, J. Z. Sun, C. C. Chi, L. S. Yu-Jahnes, A. Gupta, M. Rupp, and M. B. Ketchen, Nature (London) **373**, 225 (1995).

[8] R. R. Schulz, B. Chesca, B. Goetz, C. W. Schneider, A. Schmehl, H. Bielefeldt, H. Hilgenkamp, J. Mannhart, and C. C. Tsuei, Appl. Phys. Lett. **76**, 912 (2000).

[9] C. R. Hu, Phys. Rev. Lett. **72**, 1526 (1994).

[10] Y. Tanaka and S. Kashiwaya, Phys. Rev. Lett. **74**, 3451 (1995).

[11] A. F. Andreev, Zh. Eksp. Teor. Fiz. **46**, 1823 (1964) [Sov. Phys. JETP **19**, 1228 (1964)].

[12] M. Covington, M. Aprili, E. Paraoanu, L. H. Greene, F. Xu, J. Zhu, and C. A. Mirkin, Phys. Rev. Lett. **79**, 277 (1997).

[13] I. Iguchi, W. Wang, M. Yamazaki, Y. Tanaka, and S. Kashiwaya, Phys. Rev. B **62**, R6131 (2000).

[14] H. Aubin, L. H. Greene, Sha Jian, and D. G. Hinks, Phys. Rev. Lett. **89**, 177001 (2002).

[15] L. Alff, A. Beck, R. Gross, A. Marx, S. Kleefisch, Th. Bauch, H. Sato, M. Naito, and G. Koren, Phys. Rev. B **58**, 11 197 (1998).

[16] Satoshi Kashiwaya, Yukio Tanaka, Masao Koyanagi, Hiroshi Takashima, and Koji Kajimura, Phys. Rev. B **51**, 1350 (1995).

[17] T. Lofwander, V. S. Shumeiko, and G. Wendin, Supercond. Sci. Technol. **14**, R53 (2001).

[18] Y. Tanaka and S. Kashiwaya, Phys. Rev. B **56**, 892 (1997).

[19] Yu. S. Barash, Phys. Rev. B **61**, 678 (2000).

[20] Y. Tanaka and S. Kashiwaya, Rep. Prog. Phys. **63**, 1641 (2000).

[21] A. Gurevich and E. A. Pashitskii, Phys. Rev. B **57**, 13 878 (1998).

[22] E. Sarnelli and G. Testa, Physica C **371**, 10 (2002).

[23] B. H. Moeckly, D. K. Lathrop, and R. A. Buhrman, Phys. Rev. B **47**, 400 (1993).

[24] E. Il'ichev, M. Grajcar, R. Hlubina, R. P. J. IJsselsteijn, H. E. Hoenig, H.-G. Meyer, A. Golubov, M. H. S. Amin, A. M. Zagoskin, A. N. Omelyanchouk, and M. Yu. Kupriyanov, Phys. Rev. Lett. **86**, 5369 (2001).

[25] G. Testa, A. Monaco, E. Esposito, E. Sarnelli, D.-J. Kang, S. H. Mennema, E. J. Tarte, and M. G. Blamire, Appl. Phys. Lett. **85**, 1202 (2004).

[26] G. Wendin and V. S. Shumeiko, Phys. Rev. B **53**, R6006 (1996).

[27] M. Sigrist and T. M. Rice, J. Phys. Soc. Jpn. **61**, 4283 (1992).

[28] M. Sigrist and T. M. Rice, Rev. Mod. Phys. **67**, 503 (1995).

[29] F. Lombardi, F. Tafuri, F. Ricci, F. Miletto Granozio, A. Barone, G. Testa, E. Sarnelli, J. R. Kirtley, and C. C. Tsuei, Phys. Rev. Lett. **89**, 207001 (2002).

[30] G. Testa, A. Monaco, E. Sarnelli, A. D'Agostino, D.-J. Kang, E. J. Tarte, S. H. Mennema, C. Bell, and M. G. Blamire, Supercond. Sci. Technol. **7**, 287 (2004).

[31] A. Barone and G. Paternó, *Physics and Applications of the Josephson Effect* (Wiley, New York, 1982).

[32] H. Arie, K. Yasuda, H. Kobayashi, I. Iguchi, Y. Tanaka, and S. Kashiwaya, Phys. Rev. B **62**, 11 864 (2000).

[33] G. E. Blonder, M. Tinkham, and T. M. Klapwijk, Phys. Rev. B **25**, 4515 (1982).

[34] R. Hlubina, M. Grajcar, and E. Il'ichev, in *Studies of High Temperature Superconductors*, edited by A. V. Narlikar (Nova Science, Commack, NY, 2003), Vol. 45, p. 1.

[35] E. Il'ichev, V. Zakosarenko, R. P. J. IJsselsteijn, V. Schultze, H.-G. Meyer, H. E. Hoenig, H. Hilgenkamp, and J. Mannhart, Phys. Rev. Lett. **81**, 894 (1998).